Annals of Botany **110**: 1581–1591, 2012
doi:10.1093/aob/mcs215, available online at www.aob.oxfordjournals.org

ANNALS OF BOTANY
Founded 1887

DNA replication stress induces deregulation of the cell cycle events in root meristems of *Allium cepa*

Aneta Żabka*, Justyna Teresa Polit and Janusz Maszewski

Department of Cytophysiology, Faculty of Biology and Environmental Protection, University of Łódź, Pomorska 141/143, 90-236 Łódź, Poland
** For correspondence. E-mail zabkka@poczta.onet.pl*

Received: 1 June 2012 Returned for revision: 23 July 2012 Accepted: 22 August 2012 Published electronically: 18 October 2012

• *Background and Aims* Prolonged treatment of *Allium cepa* root meristems with changing concentrations of hydroxyurea (HU) results in either premature chromosome condensation or cell nuclei with an uncommon form of biphasic chromatin organization. The aim of the current study was to assess conditions that compromise cell cycle checkpoints and convert DNA replication stress into an abnormal course of mitosis.
• *Methods* Interphase-mitotic (IM) cells showing gradual changes of chromatin condensation were obtained following continuous 72 h treatment of seedlings with 0·75 mM HU (without renewal of the medium). HU-treated root meristems were analysed using histochemical stainings (DNA-DAPI/Feulgen; starch-iodide and DAB staining for H_2O_2 production), Western blotting [cyclin B-like (CBL) proteins] and immunochemistry (BrdU incorporation, detection of γ-H2AX and H3S10 phosphorylation).
• *Key Results* Continuous treatment of onion seedlings with a low concentration of HU results in shorter root meristems, enhanced production of H_2O_2, γ-phosphorylation of H2AX histones and accumulation of CBL proteins. HU-induced replication stress gives rise to axially elongated cells with half interphase/half mitotic structures (IM-cells) having both decondensed and condensed domains of chromatin. Long-term HU treatment results in cell nuclei resuming S phase with gradients of BrdU labelling. This suggests a polarized distribution of factors needed to re-initiate stalled replication forks. Furthermore, prolonged HU treatment extends both the relative time span and the spatial scale of H3S10 phosphorylation known in plants.
• *Conclusions* The minimum cell length and a threshold level of accumulated CBL proteins are both determining factors by which the nucleus attains commitment to induce an asynchronous course of chromosome condensation. Replication stress-induced alterations in an orderly route of the cell cycle events probably reflect a considerable reprogramming of metabolic functions of chromatin combined with gradients of morphological changes spread along the nucleus.

Key words: Chromatin, cyclin B-like proteins, DNA damage, DNA replication, γ-H2AX, histone H3 phosphorylation, hydrogen peroxide, hydroxyurea, mitosis, premature chromosome condensation.

INTRODUCTION

The large-scale changes in chromatin packaging associated with cell cycle progression produce two opposite states of nuclear DNA, one adapted to transcribe and to precisely replicate genomic sequences during interphase, and the other adjusted to distribute chromosomes into daughter cells at mitosis (Morales *et al.*, 2001). A series of transitions between up- and downstream events involved in these processes depends on checkpoint mechanisms that preserve causal ordering of specific activities and prevent cells from entering M phase before the completion of DNA synthesis and G2 functions (Hartwell and Weinert, 1989; Cools and De Veylder, 2009). Molecular components which contribute to this system create regulatory circuits keeping track of hierarchies and dependencies for making the cell cycle a one-way route composed of successive stages, each demonstrating a discrete level of nuclear organization capable of facilitating emergent tasks. As a rule, induction of signalling pathways in response to unfavourable external conditions or damaging factors combined with subsequent checkpoint activities slows down or blocks cell cycle progression, thus providing additional time needed either to supply indispensable nutrients (Van't Hof, 1985; Polit, 2009), to correct genetic lesions or to direct irreparably damaged cells towards apoptosis (Abraham, 2001; Stevens *et al.*, 2010).

Perhaps the most remarkable cell cycle control pathway conserved across all eukaryotic forms of life, the S-M checkpoint (referred to also as the DNA replication checkpoint), assembles similar biochemical elements into a three-level molecular response system composed of: (1) sensors that detect stalled replication forks or double-strand DNA breaks (DSBs), (2) specific transducers that convey appropriate signals and (3) effectors, which reply to these signals so that the cell triggers a suitable chain of events to make defence (or, alternatively, apoptotic destruction) more effective (Lukas *et al.*, 2004). An essential role for the S-M mechanism is to perceive distorted, abnormally or partially replicated DNA molecules and to prevent the assembly of active M-phase cyclin-dependent kinases (CDKs) which, together with their specific regulatory subunits (cyclins), provide the driving force for an abrupt G2-to-M phase transition. Another type of function

ascribed to the DNA-damage/S-M checkpoints relies on promoting structural changes of chromatin domains, prearranged by the phosphorylated form of H2AX histones, both to preclude far-reaching reconfigurations or potential separation of broken chromosome fragments and to facilitate access of DNA repair factors (Fernandez-Capetillo *et al.*, 2004). It is thus thought that cellular response to DNA-damaging agents must be split into two distinct yet interrelated paths capable of eliciting the downstream effects on both replication sites and those components which trigger the onset of nuclear division. Accordingly, a broad variety of genomic lesions and mutations that disrupt crucial functions of the checkpoint response system have been shown to accelerate mitotic events, leading cells with damaged or unreplicated DNA to premature chromosome condensation (PCC; Elledge, 1996; Nghiem *et al.*, 2001).

Recent experiments using continuous incubations of *Allium cepa* root meristems with low concentrations of hydroxyurea (HU) provided evidence that long-term exposure to replication stress disrupts essential links of the S-M dependency mechanisms, leading cells either to PCC or to an uncommon form of chromatin condensation, establishing biphasic organization of cell nuclei with both interphase and mitotic domains of chromatin (Żabka *et al.*, 2010). The emergent structures can be seen as a product of polarized accumulation of cyclin B-like (CBL) proteins which spread along successive regions of the perinuclear cytoplasm. It has been hypothesized that, by forming gradients, an increased concentration of these proteins helps to define activation centres for CDKs, which results in an abnormal pattern of mitotic condensation and its possible consequent effects.

Two major aspects have been selected for the current study to assess conditions that compromise checkpoint controls and convert DNA replication stress into an abnormal course of the cell cycle. The first, relating to what might be called 'a systemic response', includes wide-ranging reactions shared by almost all root tip cells exposed to prolonged HU treatment. The other problem refers to a group of enlarged cells which display either prematurely condensed chromosomes or half interphase/half mitotic (IM) nuclear structures. Immunofluorescence observations indicate that emergent biphasic nuclei are preceded by an early phosphorylation of H3 histones. Furthermore, cell nuclei which commence S phase show gradients of BrdU (bromodeoxyuridine) labelling, suggesting a polarized distribution of factors needed to reinitiate functioning of stalled replication forks arising secondary to HU-induced depletion of deoxyribonucleoside diphosphates (dNTPs).

MATERIALS AND METHODS

Plant material

Seeds of *Allium cepa* (obtained from a horticulture farm in Lubiczów) were sown on moist paper sheets and germinated in the dark at 20 °C. Four days after imbibition, seedlings with primary roots reaching 1·5–0·2 cm were sterilized in 0·1 % acetone/chloroform for 30 min, washed several times with distilled water and cultivated on blotting paper in Petri dishes (Ø 6 cm) filled with 10 mL of either distilled water (control samples) or 0·75 mM HU solution (for 24–72 h, at 20 °C, in the dark). Biphasic (IM) cells showing gradual changes of chromatin condensation were obtained following continuous 72 h treatment of seedlings with 0·75 mM HU (without renewal of the medium). During incubations, roots were permanently aerated by gentle rotation of Petri dishes in a water-bath shaker (100 r.p.m.).

Feulgen staining

Excised primary root tips of *A. cepa* were fixed in cold Carnoy's mixture (absolute ethanol and glacial acetic acid; 3:1, v/v) for 1 h, washed several times with ethanol, rehydrated, hydrolysed in 4 M HCl (1 h), and stained with Schiff's reagent (pararosaniline) according to the standard method (Polit *et al.*, 2002). After rinsing in SO_2-water, 1·5-mm-long apical segments were cut off, washed in distilled water, placed in a drop of 45 % acetic acid and squashed onto slides. Following freezing with dry ice, coverslips were removed, and the dehydrated dry slides were embedded in Canada balsam before examination.

H_2O_2 detection

The generation of H_2O_2 was observed using: (1) iodide starch (IS) staining (according to Barceló, 1998; Urs *et al.*, 2006) and (2) DAB (3,3-diaminobenzidine) uptake (according to Thordal-Christensen *et al.*, 1997), with minor modifications of both methods. For IS staining, seedlings briefly soaked (1 min) in 1 mM ascorbic acid (AA) to remove endogenous H_2O_2 were immersed for 8 h in 4 % (w/v) starch/0·1 M KI (adjusted to pH 5·0 with KOH) mixture dissolved either in distilled water (control) or in 0·75 mM HU (HU-treated plants). Production of H_2O_2 was monitored under the microscope by observing brown-stained areas developing on the cut surface of hand-made longitudinal sections of root tips. To detect H_2O_2 by means of DAB polymerization, roots were plunged in Tris-buffered (10 mM Tris, 10 mM EDTA-2Na, 100 mM NaCl) DAB-HCl (1 mg ml^{-1}; pH 7·5) dissolved in distilled water (control), 0·75 mM HU (HU-treated plants) or 0·75 mM HU solution supplemented with 1 mM AA. Following 16-h incubations, excised 1·5-mm root tips were fixed for 45 min (20 °C) in PBS-buffered 3·7 % paraformaldehyde, washed several times with PBS, and placed in a citric acid-buffered 2·5 % pectinase (pH 5·0; 37 °C for 45 min). Digested root meristems were washed with PBS and squashed onto microscope slides in a mixture of glycerol and PBS (9 : 1; v/v). H_2O_2 was visualized under the microscope as a reddish-brow coloration of the cells.

Immunocytochemical detection of γ-phosphorylated H2AX and phosphorylated H3 (Ser10) histones

Detection of γ-phosphorylated H2AX histones was carried out according to the method described by Rybaczek and Maszewski (2007*a*) and Rybaczek *et al.* (2007), and, in general, the same procedure was applied in assays used for H3 phosphorylation at a conserved serine 10 residue (H3S10Ph). Briefly, excised 1·5-mm-long apical parts of roots from the control and HU-treated seedlings were fixed for 45 min (20 °C) in PBS-buffered 3·7 % paraformaldehyde

and, after washing with PBS, placed for 45 min (37 °C) in a citric acid-buffered digestion solution (pH 5·0) containing 2·5 % pectinase (Fluka, Germany), 2·5 % cellulase (Onozuka R-10; Serva, Heidelberg, Germany) and 2·5 % pectolyase (ICN, Costa Mesa, CA, USA). After rinsing with PBS and distilled water, root tips were squashed onto slides. Air-dried slides were pretreated with PBS-buffered 8 % bovine serum albumin (BSA) and 4 % Triton X-100 at 20 °C for 50 min and, depending on the experimental series, incubated for 12 h in a humidified atmosphere (4 °C) with rabbit polyclonal antibody raised against human H2AX histones phosphorylated at Ser139 (Upstate Biotechnology, Lake Placid, NY, USA) at a dilution of 1 : 750 (Rybaczek and Maszewski, 2007*b*) or with rabbit polyclonal antibody raised against human H3 histones phosphorylated at Ser10 (1:500; Sigma-Aldrich, Poznan, Poland), each dissolved in PBS containing 1 % BSA. After washing with PBS, slides were incubated for 1·5 h (20 °C) with secondary goat anti-rabbit IgG [F(ab′)2 fragment] FITC antibody (1 : 500; Sigma-Aldrich) in PBS (1 : 500) and counterstained with DAPI (4′,6-diamidino-2-phenylindole; 0·4 μg mL^{-1}, for γ-H2AX) or with PI (propidium iodide; 0·3 μg mL^{-1}, for H3S10Ph). Slides washed with PBS were air dried and embedded in a PBS/glycerol mixture (9 : 1) with 2·3 % diazabicyclo[2·2.2]octane (DABCO).

Western blot analysis with anti-cyclin B1 antibody

CBL mitotic proteins were analysed by Western blotting as described previously (Żabka *et al.*, 2010). Root meristem cells were lysed using a P-PER Plant Protein Extraction Kit (Pierce, Rockford, IL, USA) supplemented with Protease Inhibitor Cocktail (Sigma-Aldrich) according to the supplier's instructions. The samples were cleared by centrifugation, and total protein extracts, fractionated on 4–12 % Bis Tris/2-(4-morpholino)-ethanesulfonic acid SDS-NuPAGE Novex gel (Invitrogen Corp., Carlsbad, CA USA), were blotted onto polyvinylidene fluoride membrane (0·2-μm pore size; Invitrogen). CBL proteins were detected with the rabbit polyclonal anti-cyclin B1 IgG fraction (Sigma-Aldrich) diluted to 1 : 300 using the Chromogenic Western Blot Immunodetection Kit (Invitrogen). Band intensities of CBL proteins were quantified by densitometry.

DNA replication assay with BrdU

To preserve whole root meristem cells, a procedure avoiding nuclear isolation was developed. Control and HU-treated seedlings were pulsed for 45 min with 30 μM BrdU solution at 20 °C in the dark. Excised 1·5-mm-long meristems were then washed with ice-cold Tris buffer [10 mM Tris (hydroxymethyl)-aminomethane, 10 mM EDTA-2Na, 100 mM NaCl, pH 7·2) for 5 min and fixed for 40 min at 4 °C in freshly prepared 4 % paraformaldehyde. After fixation, root tips thoroughly washed with distilled water were placed in a citric acid-buffered digestion solution (as for detection of γ-H2AX and H3S10Ph) and incubated for 15 min at 37 °C. Subsequently, root tips were washed again, squashed onto slides and treated with 1·5 M HCl for 1·5 h at 25 °C for partial denaturation of nuclear DNA. After washing with Tris buffer containing 0·5 % Triton X-100, mouse monoclonal anti-BrdU antibodies (Sigma-Aldrich) diluted in Tris buffer (1 : 50) were added. Following an overnight incubation at 4 °C, slides were washed in Tris buffer (10 min, three times) and incubated for 1 h with FITC-conjugated goat anti-mouse monoclonal antibodies (Sigma-Aldrich) diluted 1 : 500 in Tris buffer (25 °C; wet dark chamber), washed twice (10 min each) in Tris buffer and embedded in a PBS/glycerol mixture (9 : 1) with 2·3 % DABCO.

Microscopic measurements, observations and analyses

Micrographs of Feulgen- and DAB-stained cells were made under a Optiphot-2 microscope (Nikon, Tokyo, Japan) equipped with phase contrast optics and DXM 1200 CCD camera. Cell length was measured using Lucia Image Analysis System (version 4·6). Immunofluorescence of γ-H2AX, H3S10Ph and BrdU-labelled cells was observed under an Eclipse E-600 fluorescence microscope (Nikon), equipped with U2 filter (UVB light $\lambda = 340–380$ nm) for DAPI, B2 filter (blue light $\lambda = 465–496$ nm) for FITC, or G2 filter (green light; $\lambda = 540/25$ nm) for PI-stained cell nuclei. The cell cycle positions were estimated by microfluorimetric analysis of nuclear DNA content after PI or DAPI staining. All images were recorded at exactly the same time of integration using a DS-Fi1 CCD camera (Nikon). Quantitative measurements of BrdU-, DAPI- and PI-labelled nuclear DNA immunofluorescence were made after converting colour images into greyscale and expressed in arbitrary units as mean pixel value (pv) spanning the range from 0 (dark) to 255 (white) according to described methods (Rybaczek *et al.*, 2007; Żabka *et al.*, 2010). All immunofluorescence analyses were repeated at least twice, Western blot assays were made in triplicate and other experiments were repeated several times. The total number of analysed cells for one set of data was always more than 1000, if not indicated otherwise.

RESULTS AND DISCUSSION

HU-mediated replication stress is correlated with H_2O_2 production and generation of phospho-H2AX foci

The enzymatic conversion of ribonucleoside diphosphates (NDPs) to the corresponding dNTPs, carried out by a tetrameric ribonucleotide reductase (RNR), is a prerequisite for establishment of the balanced quantities of precursors required for all DNA synthesis and DNA repair processes (Chabes and Thelander, 2000). By quenching the catalytically essential tyrosyl R2 radical of RNR, HU prevents cells from traversing the S-phase and accounts for a number of S-phase defects, including an enhanced production of replication intermediates with long single-stranded DNA regions, DSBs and inappropriate processing of the backed-up replication forks (Camier *et al.*, 2007).

In addition to DNA lesions induced by stalled replication forks, HU can also generate site-specific DNA-damage by creating hydrogen peroxide (H_2O_2) and/or nitric oxide (Sakano *et al.*, 2001). To assess whether and, if so, to what extent H_2O_2 accumulates in HU-treated roots of *A. cepa*, two simple histochemical tests were carried out (Fig. 1). The first, based on iodine-starch (IS) staining after the hydrogen

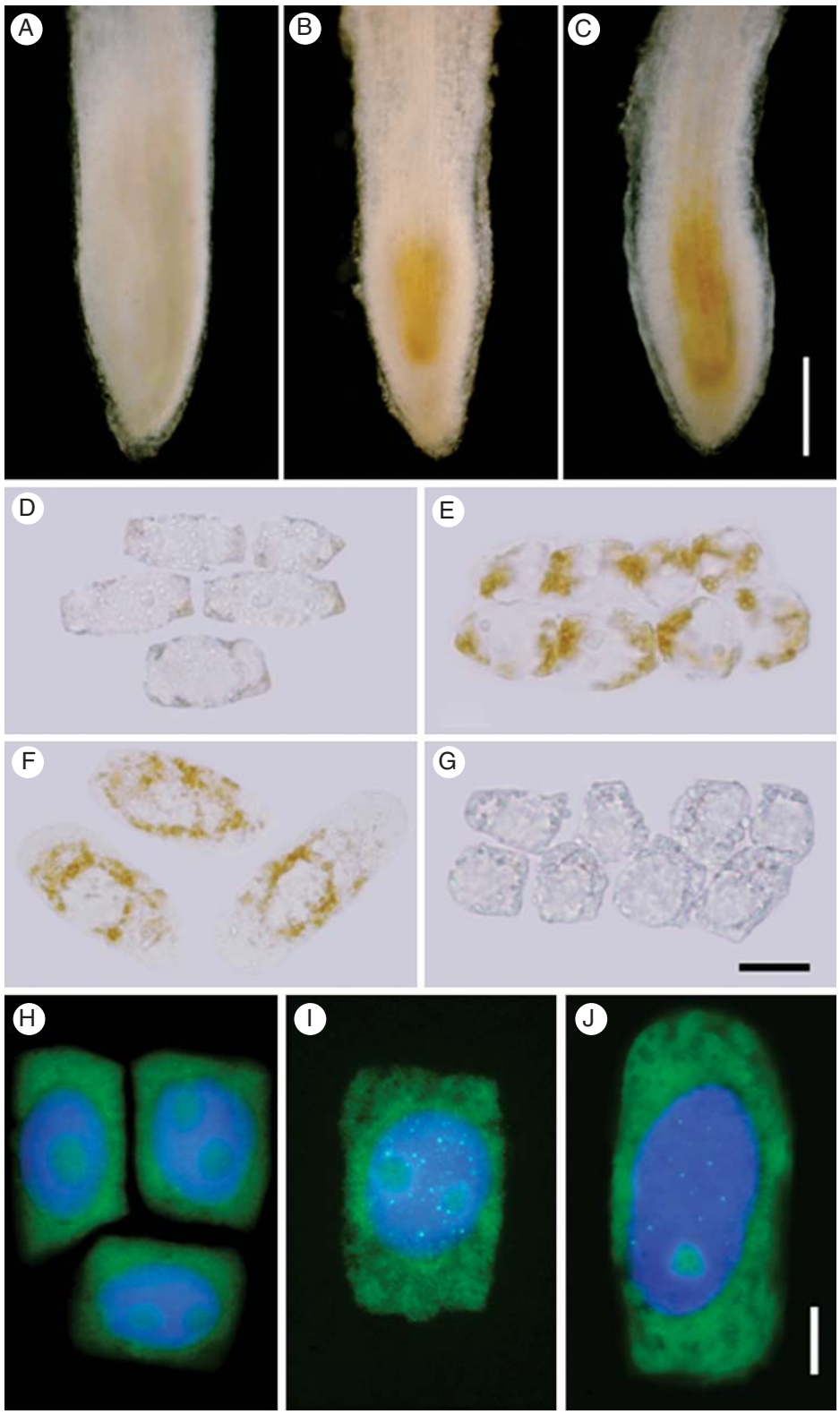

FIG. 1. DNA replication stress-induced generation of H_2O_2 (A–G) and γ-H2AX foci (H–J) in root meristems of *A. cepa* treated with 0·75 mM HU. (A–C) Hand-made longitudinal sections of root tips stained using the iodide-starch (IS) method in (A) the control seedling, and following (B) 24 h and (C) 72 h HU treatment. Scale bar = 500 μm. (D–G) DAB-stained cells in root meristems from (D) control roots, (E) after 24 h, (F) 72 h HU treatment and (G) from seedlings incubated for 24 h with a mixture of 0·75 mM HU and 1 mM ascorbic acid. Scale bar = 20 μm. (H–J) Immunofluorescence of γ-phosphorylated H2AX foci (bright) formed in cell nuclei from (H) the control roots, (I) after 24 h and (J) after 72 h replication stress induced by HU. Nuclear DNA counter-stained with DAPI. Scale bar = 10 μm.

peroxide-mediated oxidation of iodide ions (according to Olson and Varner, 1993; Fig. 1A–C), revealed a narrow darkening region at the tip of the root, which after a 24 h incubation with HU covered the centre of the meristem and extended acropetally in files of cells throughout a distance of about 0·6 mm (Fig. 1B). Increasing incubation times resulted in a fairly sharp IS staining expanded over a broader profile area of the longitudinal section, reaching the boundaries of cell layers predestined to differentiate into root cortex (Fig. 1C). Although the second method, using DAB polymerization into reddish-brown deposits (originally developed by Frederick, 1987), yielded essentially the same macroscopic result (due to strong staining of the epidermal layer), it proved to be a useful quantitative measure of cells showing H_2O_2-dependent sites of intense peroxidase activity (Fig. 1D–G). As compared with the frequency of DAB-stained cells in the control plants (8·6 %; Fig. 1D), the incidence of such cells in root tips of *A. cepa* seedlings incubated for 24 (Fig. 1E) and 48 h with 0·75 mM HU increased to 79·8 and 91·3 %, respectively, and to more than 96 % of the whole cell population after the 72-h treatment (Fig. 1F). No DAB polymers could be seen in roots treated with HU/AA mixture (Fig. 1G).

Despite significant variation in developmental traits between different groups of multicellular organisms, most of the genetic and epigenetic factors that contribute to the cell cycle regulatory networks are likely to be similar in plants and their animal or yeast counterparts. The high degree of amino acid sequence homology among proteins which serve as components of these pathways reflects an evolutionary ancient mechanism comprising sensor kinases related to phosphoinositide 3-kinases (PIKKs), ATM and ATR, which perceive DNA damage or replication block, respectively (reviewed by Abraham, 2001), and DNA-dependent protein kinase (DNA-PK) indispensable for the repair of DSBs (Block *et al.*, 2004). Recent immunocytochemical analyses have shown that ATM/ATR-mediated phosphorylation of H2AX at the C-terminal Ser-Gln-Glu sequence constitutes one of the earliest responses to HU-induced DNA damage in three plant species differing with respect to DNA content and chromatin structure: *Allium porrum*, representing a reticulate type of DNA package; *Vicia faba*, having semi-reticulate cell nuclei; and *Raphanus sativus*, characterized by a chromocentric type of chromatin (Rybaczek and Maszewski, 2007*a*). The current immunocytochemical study indicates that the frequency of cell nuclei carrying phoshpho-H2AX foci at late stages of interphase (with DNA contents around the 4C value; Fig. 1H–J) increases from 2·7 % in the control root meristems of *A. cepa* to only about 6–7 % (depending on the incubation period) in HU-treated seedlings (Table 1). Similarly to *A. porrum* (but in contrast to *V. faba* and *R. sativus*), distinct fluorescing H2AX foci have been found evenly scattered over the whole area of chromatin with no preference to either perinucleolar regions or chromocentres (Fig. 1I, J). The estimated mean number of discernible phospho-H2AX foci increased from fewer than one in the control cell nuclei to above 16 after 24 h of HU treatment and to fewer than seven after the next 2 d of prolonged replication stress (Table 1). According to Rybaczek and Maszewski (2007*b*), a fairly low number of DNA damage sites marked by immunofluorescent aggregates of phospho-H2AX corresponds well with the compact structure of chromatin, which renders it both resistant to DSBs and/or less accessible to molecular elements that arrange the cell cycle checkpoint and DNA repair functions.

Prolonged replication stress leads to premature chromosome condensation and creates biphasic interphase-mitotic cell nuclei

A series of recent studies have shown that long-term incubations of primary roots of *A. cepa* with low doses of HU (at concentrations decreasing from 0·75 to 0·5 mM) give rise to a considerable degree of diversity among root meristem cells, with a dominant S/G2 fraction and a small population of M-phase cells displaying either evident symptoms of premature chromosome condensation (PCC-cells) or an unusual biphasic phenotype with IM nuclear structures (Żabka *et al.*, 2010). Accordingly, a significant increase in the frequency of interphase cells has been interpreted as a secondary effect of the block imposed upon DNA synthesis. Thus, the persistent occurrence of aberrant mitotic structures was considered as a consequence of mechanisms which allow some of the root meristem cells to escape the DNA stress-response pathway and to continue the cell division cycle regardless of the incomplete replication of nuclear DNA (Rybaczek and Maszewski, 2007*a*; see also Kohn *et al.*, 2002).

As with previous observations made following alternate 0·75/0·5 mM HU treatments (Żabka *et al.*, 2010), the current experiments show that continuous 72 h incubation of *A. cepa*

TABLE 1. *Hydroxyurea-induced effects in root meristems of* Allium cepa

Experimental series	Control	Duration of HU treatment		
		24 h	48 h	72 h
Induction of nuclear γ- H2AX foci				
Percentage of G2-cells* with nuclear γ-H2AX foci	2·7 ± 0·8	6·8 ± 1·4	6·1 ± 1·5	5·7 ± 1·8
Mean number of γ-H2AX foci/nucleus (G2-cells)	0·8 ± 0·3	16·4 ± 1·5	10·3 ± 1·2	6·5 ± 1·2
Dynamics of root growth				
Mean daily root growth rate (mm/24 h)	8·4 ± 0·8 (24^{th} h) to 7·0 ± 0·9 (72^{nd} h)	7·7 ± 1·4	2·7 ± 0·6	1·2 ± 0·5
Mean length of root meristem (μm)	927 ± 64	760 ± 107	555 ± 127	373 ± 94
Mean number of cells per meristem	12 115 ± 1295	5590 ± 1177	5181 ± 1023	4096 ± 105
Mean cell length (μm)	27·2 ± 13·6	32·2 ± 14·5	37·2 ± 16·6	42·8 ± 19·6

* Position of cells in interphase was determined by microfluorimetric measurements of DAPI-stained nuclei.

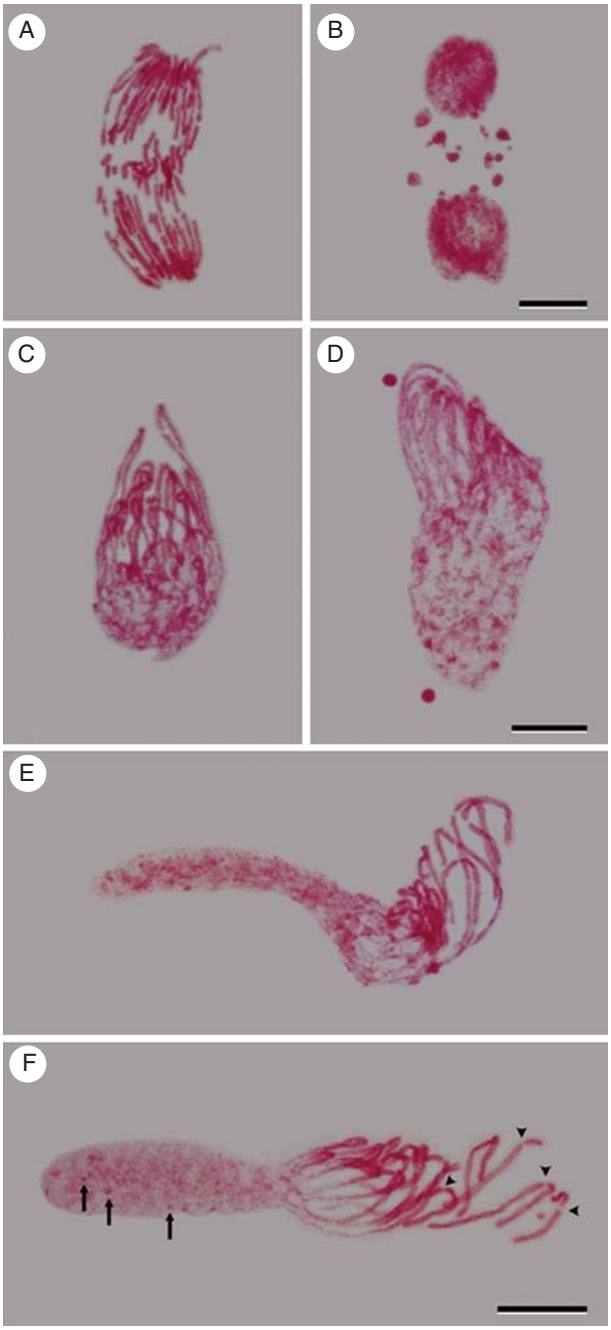

FIG. 2. Nuclear Feulgen-staining of *A. cepa* root meristem cells following 72 h treatment with 0·75 mM HU. (A, B) Symptoms of PCC during (A) anaphase and (B) late telophase. (C–F) Intrachromosomal asynchrony observed during transitions from (C, D) early-to-late prophase and (E, F) interphase-to-prophase/prometaphase, both with evident gradients of chromatin condensation. Darkly stained chromocentres corresponding to telomeric heterochromatin are indicated by arrows, and chromosomal constrictions by arrowheads. Scale bars = 20 μm.

root meristems with 0·75 mM HU (without renewal of the medium) results in a fraction of PCC-cells showing chromosomal breaks, acentric fragments, lagging chromatids and micronuclei (Fig. 2A, B), accompanied by a number of cells displaying biphasic IM nuclear organization with gradients of condensing chromatin (Fig. 2C–F). The inclusive nature

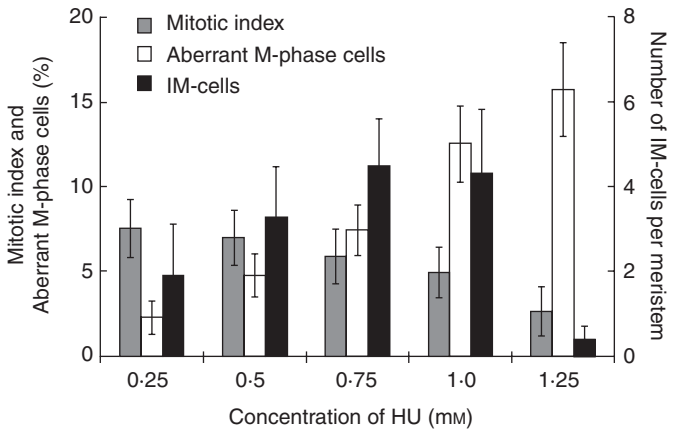

FIG. 3. The effect of various concentrations of HU (72 h incubation) on the mitotic index (%), fraction of aberrant M-phase cells (%) and number of IM-cells with intranuclear asynchrony of chromatin condensation. Means were calculated for ten root meristems (>1500 cells per meristem).

of these gradients depends on the range of the cell cycle stages straddling opposite sides of the nucleoplasm, with the extreme cases where an assembly of condensed and decondensed chromatin adjoined by a short transition region creates an extraordinary 'octopus-like' structure bearing numerous chromosomal arms sticking out of the interphase nuclear body (Fig. 2E, F). To evaluate any possible relationship between the strength of the replication stress and the ability of cells to abrogate the 'safeguard' system designed by the S-M checkpoint control mechanism, root meristems were continuously exposed to various concentrations of HU. Both mitotic activity and chromosomal aberrations (percentage of M-phase cells with PCC or with biphasic IM nuclear morphology) were recorded after 72 h of incubation. The results of this analysis clearly demonstrate an inverse correlation between the dose-dependent reduction in the frequency of mitotic cells and an increase in relative number of aberrant chromosomal structures (Fig. 3). However, while the PCC index grew steadily with increasing concentration of HU, the incidence of biphasic cell nuclei (expressed as the mean number of IM events per root meristem) reached peak values of about four in seedlings exposed to 0·75 mM HU (chosen for all further experiments) and to 1 mM HU, and then decreased at the highest tested concentration (1·25 mM).

Replication stress brings about apparent time-dependent alterations in the structure and activity of root meristem cell populations in *A. cepa* (Table 1). Mean growth rate of the primary roots decreased slightly within the first 24 h of treatment and then slowed significantly after 48 and 72 h of treatment. Consistent with the reduced elongation rates, the total number of root apical cells diminished considerably, resulting in a sharp reduction in meristem size. Although initially (24- and 48-h periods) the mitotic index decreased to some extent, it increased after 72 h, probably due to checkpoint adaptation that allows some of the cells to continue the cell cycle regardless of the existing damage (Bartek and Lukas, 2007). The mean profile surface area of root meristem cells enlarged remarkably, reaching more than twice the values recorded in the untreated root samples. The distribution patterns of cell lengths (Fig. 4) show that the population of

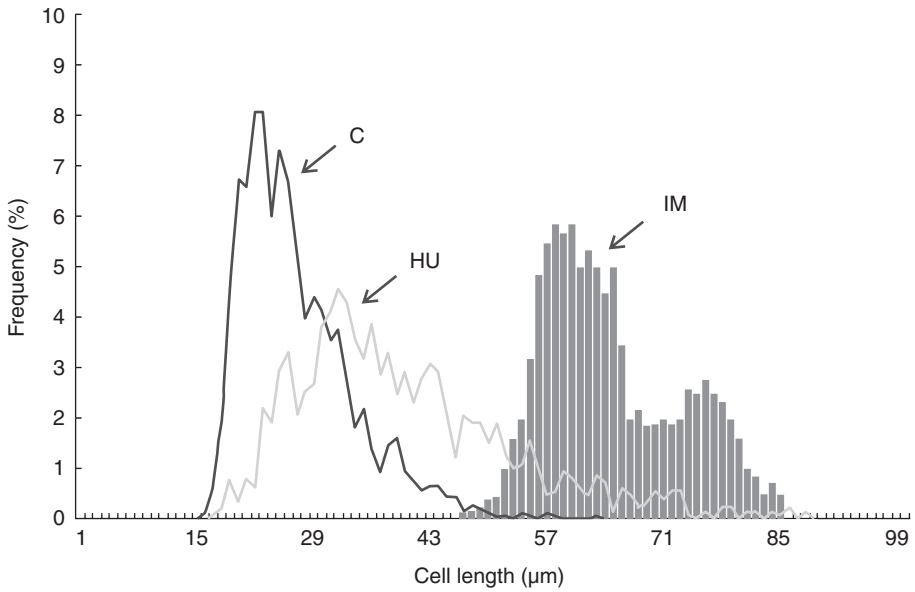

FIG. 4. Frequency distribution patterns (%; histogram profiles) of cell lengths (μm) in root meristems of *A. cepa*: control (C) and 0·75 mM HU-treated seedlings (HU; 72 h incubation). For each plot, $n > 1500$. The grey histogram (IM) shows the frequency distribution pattern for IM-cell lengths; $n = 100$.

biphasic cells does not overlap the range of the largest cells noted in the control plants. Consequently, the data obtained suggest that a certain minimum cell size must be attained to establish spatial conditions favourable for the development of asynchronous IM nuclear structures with both decondensed and condensed parts of chromatin.

Increased level of CBL proteins abrogates cell cycle checkpoints

The timed activation of the CDKs is regulated by phase-specific expression and degradation of their cyclin components (Pines and Rieder, 2001). In most eukaryotes including higher plants, B-type cyclins appear at G2/M phase and become degraded using ubiquitin-protein ligase (anaphase-promoting complex/cyclosome; APC/C) to decrease CDK activity prior to spindle degradation, chromosome decondensation, nuclear envelope reformation and cytokinesis (Weingartner *et al.*, 2004; Francis, 2009). Quantitative immunofluorescence measurements of root tip cells of *A. cepa* exposed to long-term incubation with 0·75/0·5 mM HU (Żabka *et al.*, 2010) have shown a considerable increase in the amount of CBL proteins, exceeding by more than 60 % the maximum levels observed in late G2- and M-phase cells from control plants. In addition, a significant number of elongated cells revealed evident gradients of these proteins spread along successive regions of the perinuclear cytoplasm. To support our earlier immunocytochemical results, protein extracts from equal fresh weight samples of 1·5-mm-long root tips were scored every 24 h of HU treatment, immunoblotted for CBL proteins and quantified by optical density measurements. The data in Fig. 5 show that 24 h incubation with 0·75 mM HU induces an increase in the amount of CBL proteins, followed by a gradual decline at later periods of incubation (after 48 and 72 h). However, taking into account progressive reduction in the number of cells found in HU-treated root meristems (see Table 1), the

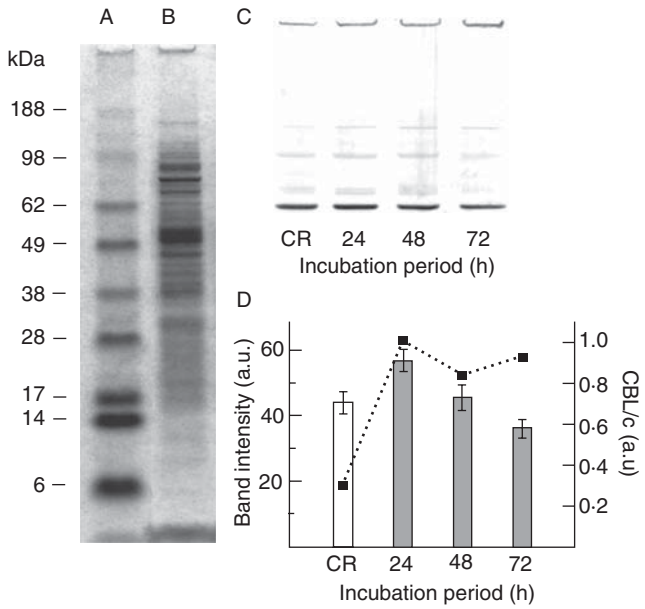

FIG. 5. Immunoblotting of CBL proteins in lysates of *A. cepa* root meristem cells. (A) Molecular weight marker, (B) SDSNuPAGE electrophoresis and Coomasie staining, (C) Western blot of proteins extracted from the control roots (CR) and after successive periods of incubation with 0·75 mM HU. (D) Intensities of bands shown in (C), quantified by densitometry; a.u. = arbitrary units. Values represent means ± s.d. for three independent determinations. The dotted line illustrates relative changes in the content of CBL proteins per cell (CBL/c), evaluated as a ratio of mean band intensity to mean number of cells estimated in root meristem from the control roots (CR) and after successive periods of incubation with HU (cell counts given in Table 1).

average content of CBL proteins per cell is about three times higher than that estimated for the untreated plants and remains almost unchanged throughout the whole 72-h period of replication stress. Accordingly, our current results strongly support our previous hypothesis suggesting that there may be

a direct link between the effects of HU-mediated deceleration of S- and G2-phase transitions, an enhanced accumulation of CBL proteins and, consequently, an overactivation of CDK complexes which, together with some unidirectional mitotic stimuli, might account for an abnormal (polarized) condensation of chromosomes.

HU-mediated deregulation of nuclear DNA replication

By comparing experimental data designed to investigate DNA replication in plant and mammalian cells, a number of common aspects concerning nuclear organization have been identified that seem to reflect some important elements in nuclear structure–function relationships among eukaryotes. The principal feature of chromosomal DNA biosynthesis is that replicons function in groups and the timing of their sequential activation during S-phase, at least in part, depends on the chromatin state in which replication origins reside (Weinreich *et al.*, 2004; Zink, 2006; Aladjem, 2007). Consistently, a precise temporal pattern of DNA replication occurs at a limited number of discrete foci localized within successive large-scale chromatin domains of the nucleus. In general, decondensed regions of chromatin containing transcriptionally competent and active genes (euchromatin) replicate during early to mid S-phase, while transcriptionally silent regions of condensed heterochromatin replicate later, during the second half of the S-phase (Gilbert, 2002; Ding and MacAlpine, 2011). A heterogeneous distribution of replication foci within different nuclear compartments during interphase reveals the Rabl orientation of the chromosomes, with centromeres and telomeres clustered at opposite poles of the nucleus (Samaniego *et al.*, 2002).

To detect possible effects of prolonged HU treatment on the spatial distribution of replication foci, root tip cells of *A. cepa* released from the block were pulse-labelled with BrdU and processed for indirect anti-BrdU immunofluorescence staining (Fig. 6). In the control and HU-pretreated plants, more than one-third and more than three-quarters of cells, respectively, had BrdU-labelled nuclei, some of them showing a polar distribution of fluorescence (Fig. 6A, B). In root meristems treated for 72 h with 0·75 mM HU (but not in the control plants), about 1·3 % of BrdU-positive nuclei revealed a gradual change in the intensity of immunostaining extending through successive regions of chromatin. Concurrently, an uneven distribution of active DNA replication sites along the major axes of the nuclei was clearly distinct from the labelling pattern observed in late S-phase nuclei showing bipolar Rabl alignment of large fluorescing foci confined to centromeres

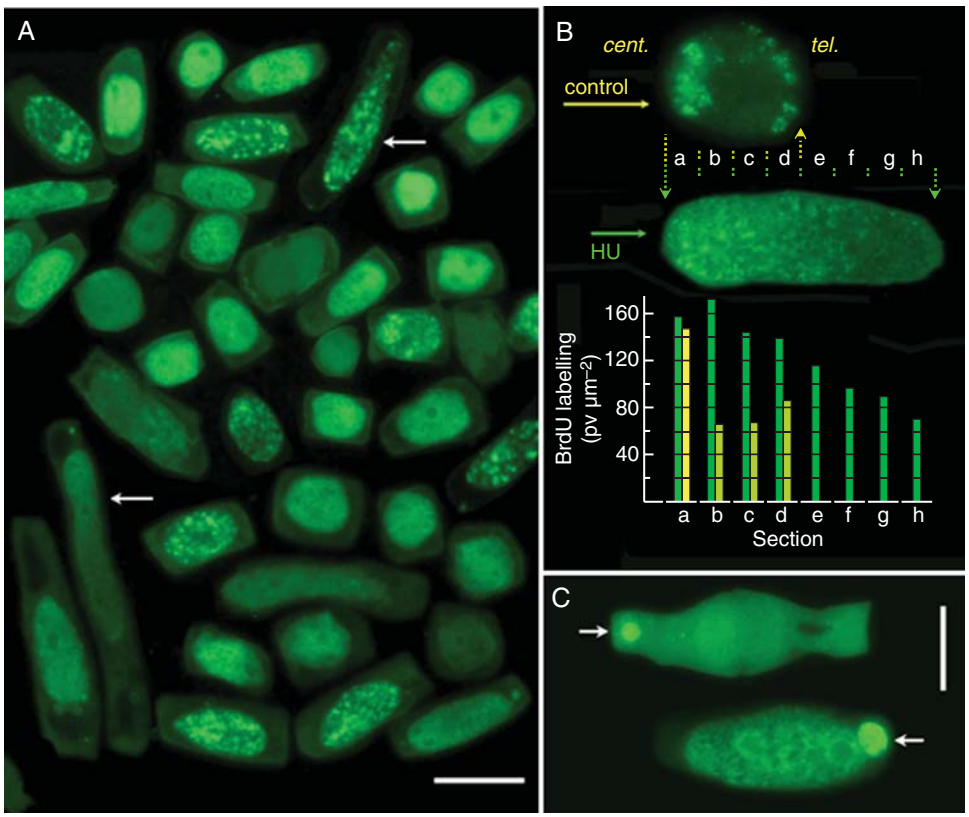

FIG. 6. Immunofluorescence of BrdU-labelled nuclei in root meristem cells of *A. cepa*. (A) Population of root tip cells resuming DNA replication after 72 h incubation with 0·75 mM HU. Arrows point to nuclei displaying gradients of BrdU incorporation. Scale bar = 50 µm. (B) Comparison of BrdU-labelling patterns in cell nuclei showing centromeric (*cent.*) and telomeric (*tel.*) regions of late replicating heterochromatin separated according to Rabl configuration (control), and the gradient of BrdU incorporation into chromatin resuming DNA synthesis after 72 h of HU-induced replication stress (HU). Diagrams show mean intensities of BrdU-immunolabelling [pixel values µm^2 (pel/µm^2)] evaluated in four (control; values in yellow) and eight (pretreatment with HU; values in green) successive nuclear sections (a–d and a–h; respectively). Section length = 8 µm. (C) Asynchronous DNA replication in micronuclei (arrows) neighbouring polar regions of aneuploid cell nuclei in elongated root meristem cells pretreated with HU and post-incubated with BrdU. Scale bar = 20 µm.

and telomeres (Fig. 6B). Moreover, some cells revealed evident asynchrony of BrdU incorporation between aneuploid nuclei and complementary micronuclei localized at the polar regions of the cytoplasm (Fig. 6C). In each case, a gradual change in the immunofluorescence might be attributed solely to the large cells, with a major to minor axis ratio greater than 3 : 1. Seemingly, there is a subtle variation in the cytoplasmic environment at both poles of the elongated cell. This may be required to support the formation of biphasic IM nuclei, and also may impose conditions responsible for gradual replication of nuclear DNA during the reprogrammed passage through S-phase. It is not our intention, however, to postulate any causal interconnection between the two phenomena.

Histone H3 phosphorylation extended in time and scale

The spatio-temporal regulation of template DNA replication correlates with chromatin conformation, DNA methylation and a number of post-translational modifications of histones (McNairn and Gilbert, 2003; Göndör and Ohlsson, 2009; Kundu and Peterson, 2009). Among the last-named, phosphorylation at a conserved serine residue (Ser10) in the N-terminal tail of histone H3 (H3S10) is thought to be correlated with the initial stages of chromatin condensation during mitosis and meiosis (Wei *et al.*, 1998; Nowak and Corces, 2004). In vertebrates, H3S10 phosphorylated by Aurora B kinase (Crosio *et al.*, 2002) occurs early in G2-phase primarily within pericentromeric heterochromatin and then spreads along the chromosome arms as mitosis proceeds. In plants, mitotic H3S10 phosphorylation starts later (at prophase) and does not extend beyond the pericentric region (Houben *et al.*, 1999; Manzanero *et al.*, 2000).

Biphasic IM-cells reveal bent chromosomes developing at the mitotic pole of each nucleus, some of them supplied with constrictions (Fig. 2F; arrowheads). Concurrently, the remaining part of interphase chromatin shows densely stained chromocentres (Fig. 2F; arrows). To test whether such an arrangement indicates a defined polarity of the nucleus (according to the Rabl configuration), root meristem cells of *A. cepa* were immunolabelled with an antibody against phosphorylated H3S10 (H3S10Ph). As expected, each IM-cell has exposed a row of fluorescent areas representing pericentromeric regions at the most condensed segments of the emergent chromosomes (Fig. 7A, B). Surprisingly, however, and in contrast to the control seedlings (Fig. 7C, E, G), HU-treated meristem cells showed strong immunolabelling of H3S10Ph not only in the periods ranging from early prophase to ana-telophase, but also in the G2-phase and in late telophase (Fig. 7D, F, H–J). A significant number of large cells with nuclear DNA contents around the 4C value (nearly three-fifths of all G2 cells) demonstrated distinct clusters of immunofluorescence spots arranged in rings dispersed randomly within the nucleoplasm (Fig. 7D); their intensity of staining was slightly weaker than in prophase (Fig. 7F). In late telophase, pericentromeric immunofluorescence disappeared and new phosphorylation sites have emerged at telomeres (Fig. 7H). Thus, the prolonged HU treatment has been found to extend both the relative time span and the spatial scale of H3S10 phosphorylation, as compared with the control plants. Similar effects have been observed previously in root meristems of *Trillium camschatcense* as a result of cold treatment (Manzanero *et al.*, 2002) and in root tip cells of *A. cepa* exposed to the DNA topoisomerase I inhibitor β-lapachone (A. Żabka *et al.*, unpubl. res.). It seems possible then that additional sites of H3S10 phosphorylation are induced under stress conditions at sites of chromosomal breakage. Such a hypothesis is supported by our observation of late telophase PCC-cells showing strong H3S10Ph immunofluorescence of broken chromatids aligned in the equatorial plane of the cell (Fig. 7I, J). Seemingly, most of these fragments represent telomeric parts of acentric chromatids, initially lost during aberrant anaphase and then passively arranged in a row by phragmoplast microtubules. Our assumption is consistent with immunocytochemical observations showing dynamic mitotic function of AtAurora 1 and 2 in *Arabidopsis thaliana*, which associate with the centromeres, then become translocated to the central spindle and finally converge at the phragmoplast midline along with the cell plate (Demidov *et al.*, 2005).

Conclusions

Our results indicate that the persistent replication stress imposed upon root meristems of *A. cepa* by low-dose HU treatment results in the appearance of S-phase cells with an abnormal pattern of BrdU-labelling and M-phase cells with either fragmented chromosomes (PCC-cells) or biphasic nuclei adjoining interphase and mitotic domains of chromatin (IM-cells). The formation of both cell types can be achieved by long-term incubations with increasing dilutions of HU (from 0·75 to 0·5 mM; Żabka *et al.*, 2010), or by a continuous HU treatment without intervening changing of the incubation medium (present study). Clearly, despite the enhanced production of reactive oxygen species leading to DNA damage (manifested by γ-phosphorylation of H2AX histones and chromosome aberrations), HU-mediated replication stress does not affect transcription and allows the cells to keep growing despite the damaging effects of the drug. Furthermore, we conclude that the entry into PCC and the creation of biphasic IM nuclei may occur only if the amount of accumulated CBL proteins and the activity of CBL–CDK complexes reach a threshold level sufficient to override the G2 checkpoint-mediated arrest of the cell cycle. Concurrently, cell length is a determining factor by which the nucleus attains commitment to either one of two permitted ways of aberrant mitosis. In biphasic IM-cells induced by HU treatment, chromatin becomes ever more highly structured and condensed along the chromosomal axis. How the 'octopus-like' polarity of nuclear domains is regulated remains unknown. Whatever the promoting mechanism may be, there must be some interplay between appropriate signals or the inducer molecules that form subcellular morphogenetic gradients spread along the nucleus (e.g. phytohormones). Intracellularly, a precise orientation of nuclear domains with telomeres and centromeres (here shown using H3S10Ph immunofluorescence) adjusts perpendicularly to the root axis. Deregulation of the cell cycle components and the specific role of epigenetic changes in chromatin proteins remains as work in progress.

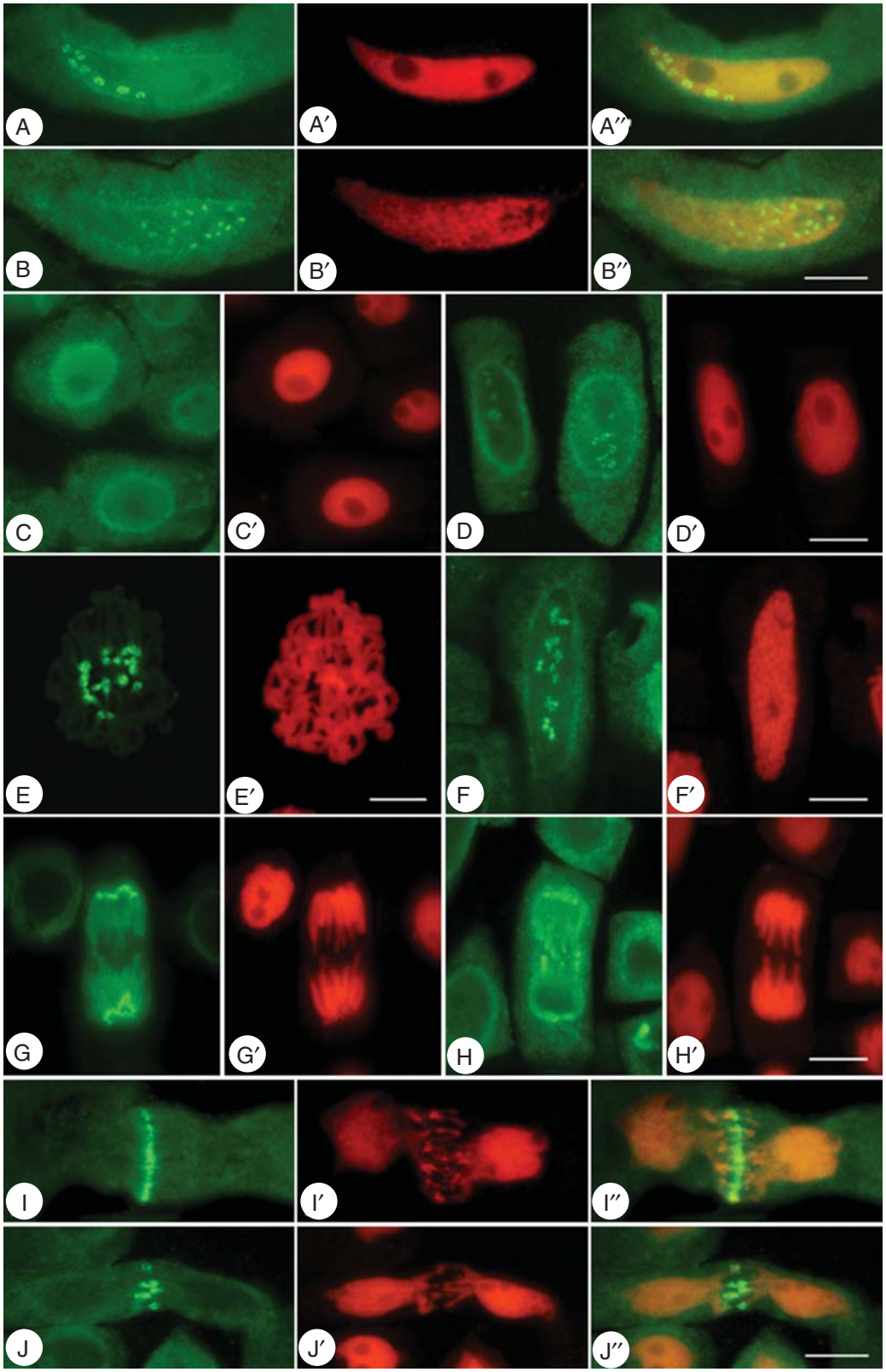

FIG. 7. Immunofluorescence of phosphorylated histone H3 (Ser10; H3S10Ph) in root meristem cells of *A. cepa*. (A, B) Polar distribution of H3S10Ph signals localized in the 'octopus-like' cell nuclei from HU-treated roots (A′, B′ – PI-stained nuclei of the same cells; A″, B″ – merged A + A′ and B + B′ images, respectively). (C, E, G) Control root meristem cells in (C) late G2 phase, (E) prophase and (G) telophase, with corresponding images of nuclear PI-staining (C′, E′, G′, respectively). (D, F, H) HU-treated root meristem cells in (D) late G2 phase, (F) prophase and (H) telophase, with corresponding nuclear PI-staining (D′, F′, H′, respectively). (I, J) H3S10Ph signals localized in fragments of chromosomes lost at the phragmoplast plate during late telophase in PCC-cells; (I′, J′) PI-stained nuclei of the same cells, (I″), (J″) – merged (I + I′) and (J + J′) images, respectively. Scale = 20 μm for each set of micrographs.

ACKNOWLEDGEMENTS

This work was supported by a grant (N N303 503038) from the National Science Centre.

LITERATURE CITED

Abraham RT. 2001. Cell cycle checkpoint signaling through the ATM and ATR kinases. *Genes & Development* **15**: 2177–2196.

Aladjem MI. 2007. Replication in context: dynamic regulation of DNA replication patterns in metazoans. *Nature Reviews Genetics* **8**: 588–600.

Barceló AR. 1998. The generation of H_2O_2 in the xylem of *Zinnia elegans* is mediated by an NADPH oxidase-like enzyme. *Planta* **207**: 207–216.

Bartek J, Lukas J. 2007. DNA damage checkpoints: from initiation to recovery or adaptation. *Current Opinion in Cell Biology* **19**: 238–245.

Block WD, Merkle D, Meek K, Lees-Miller SP. 2004. Selective inhibition of the DNA-dependent protein kinase (DNA-PK) by the radiosensitizing agent caffeine. *Nucleic Acids Research* **32**: 1967–1972.

Camier S, Ma E, Leroy C, Pruvost A, Toledano M, Marsolier-Kergoat MC. 2007. Visualization of ribonucleotide reductase catalytic oxidation establishes thioredoxins as its major reductants in yeast. *Free Radical Biology and Medicine* **42**: 1008–1016.

Chabes A, Thelander L. 2000. Controlled protein degradation regulates ribonucleotide reductase activity in proliferating mammalian cells during the normal cell cycle and in response to DNA damage and replication blocks. The Journal of Biological Chem*istry* **275**: 17747–17753.

Cools T, De Veylder L. 2009. DNA stress checkpoint control and plant development. *Current Opinion in Plant Biology* **12**: 23–28.

Crosio C, Fimia GM, Loury R, *et al* 2002. Mitotic phosphorylation of histone H3: spatio-temporal regulation by mammalian Aurora kinases. *Molecular and Cellular Biology* **22**: 874–885.

Demidov D, Van Damme D, Geelen D, Blattner FR, Houben A. 2005. Identification and dynamics of two classes of Aurora-like kinases in *Arabidopsis* and other plants. *The Plant Cell* **17**: 836–848.

Ding Q, MacAlpine DM. 2011. Defining the replication program through the chromatin landscape. *Critical Reviews in Biochemistry and Molecular Biology* **46**: 165–179.

Elledge SJ. 1996. Cell cycle checkpoints: preventing an identity crisis. *Science* **274**: 1664–1672.

Fernandez-Capetillo O, Lee A, Nussenzweig M, Nussenzweig A. 2004. H2AX: the histone guardian of the genome. *DNA Repair (Amst.)* **3**: 959–967.

Francis D. 2009. What's new in the plant cell cycle? In: *Progress in botany*, vol. 70. Lüttge U, Beyschlag W, Büdel B, Francis D**.** eds. Berlin: Springer, 33–49.

Frederick SE. 1987. DAB procedures. In: Vaughn CK**.** ed. *CRC handbook of plant cytochemistry*. Boca Raton, FL: CRC Press, 3–23.

Gilbert DM. 2002. Replication timing and transcriptional control: beyond cause and effect. *Current Opinion in Cell Biology* **14**: 377–383.

Göndör A, Ohlsson R. 2009. Replication timing and epigenetic reprogramming of gene expression: a two-way relationship? *Nature Reviews Genetics* **10**: 269–276.

Hartwell LH, Weinert TA. 1989. Checkpoints: controls that ensure the order of cell cycle events. *Science* **246**: 629–634.

Houben A, Wako T, Furushima-Shimogawara R, *et al* 1999. The cell cycle dependent phosphorylation of histone H3 is correlated with the condensation of plant mitotic chromosomes. *The Plant Journal* **18**: 675–679.

Kohn EA, Ruth ND, Brown MK, Livingstone M, Eastman A. 2002. Abrogation of the S phase DNA damage checkpoint results in S phase progression or premature mitosis depending on the concentration of UCN-01 and the kinetics of Cdc25C activation. *The Journal of Biological Chemistry* **277**: 26553–26564.

Kundu S, Peterson CL. 2009. Role of chromatin states in transcriptional memory. *Biochimica et Biophysica Acta* **1790**: 445–455.

Lukas J, Lukas C, Bartek J. 2004. Mammalian cell cycle checkpoints: signalling pathways and their organization in space and time. *DNA Repair (Amst.)* **3**: 997–1007.

Manzanero S, Arana P, Puertas MJ, Houben A. 2000. The chromosomal distribution of phosphorylated histone H3 differs between plants and animals at meiosis. *Chromosoma* **109**: 308–317.

Manzanero S, Rutten T, Kotseruba V, Houben A. 2002. Alterations in the distribution of histone H3 phosphorylation in mitotic plant chromosomes in response to cold treatment and the protein phosphatase inhibitor cantharidin. *Chromosome Research* **10**: 467–476.

McNairn AJ, Gilbert DM. 2003. Epigenomic replication: linking epigenetics to DNA replication. *Bioessays* **25**: 647–656.

Morales V, Giamarchi C, Chailleux C, *et al* 2001. Chromatin structure and dynamics: functional implications. *Biochimie* **83**: 1029–1039.

Nghiem P, Park PK, Kim Y-S, Vaziri C, Schreiber SL. 2001. ATR inhibition selectively sensitizes G1 checkpoint-deficient cells to lethal premature chromatin condensation. *Proceedings of the National Academy of Sciences, USA* **98**: 9092–9097.

Nowak SJ, Corces VG. 2004. Phosphorylation of histone H3: a balancing act between chromosome condensation and transcriptional activation. *Trends in Genetics* **20**: 214–220.

Olson P, Varner J. 1993. Hydrogen peroxide and lignification. *The Plant Journal* **4**: 887–892.

Pines J, Rieder CL. 2001. Re-staging mitosis: a contemporary view of mitotic progression. *Nature Cell Biology* **3**: E3–E6.

Polit JT. 2009. Protein phosphorylation in *Vicia faba* root meristem cells during the first steps of leaving principal control points after sucrose application. *Plant Cell Reports* **28**: 165–173.

Polit JT, Maszewski J, Kaźmierczak A. 2002. Effect of BAP and IAA on the expression of G1 and G2 control points and the G1-S and G2-M transitions in root meristem cells of *Vicia faba*. *Cell Biology International* **27**: 559–566.

Rybaczek D, Maszewski J. 2007*a*. Phosphorylation of H2AX histones in response to double-strand breaks and induction of premature chromatin condensation in hydroxyurea-treated root meristem cells of *Raphanus sativus*, *Vicia faba*, and *Allium porrum*. *Protoplasma* **230**: 31–39.

Rybaczek D, Maszewski J. 2007*b*. Induction of foci of phosphorylated H2AX histones and premature chromosome condensation after DNA damage in *Vicia faba* root meristem. *Biologia Plantarum* **51**: 443–450.

Rybaczek D, Bodys A, Maszewski J. 2007. H2AX foci in late S/G2- and M-phase cells after hydroxyurea- and aphidicolin-induced DNA replication stress in *Vicia*. *Histochemistry and Cell Biology* **128**: 227–241.

Sakano K, Oikawa S, Hasegawa K, Kawanishi S. 2001. Hydroxyurea induces site-specific DNA damage via formation of hydrogen peroxide and nitric oxide. *Japanese Journal of Cancer Research* **92**: 1166–1174.

Samaniego R, de la Torre C, Moreno Díaz de la Espina S. 2002. Dynamics of replication foci and nuclear matrix during S phase in *Allium cepa* L. cells. *Planta* **215**: 195–204.

Stevens JB, Abdallah BY, Regan SM, *et al* 2010. Comparison of mitotic cell death by chromosome fragmentation to premature chromosome condensation. *Molecular Cytogenetics* **3**: 20.

Thordal-Christensen H, Zhang Z, Wei Y, Collinge DB. 1997. Subcellular localization of H_2O_2 in plants: H_2O_2 accumulation in papillae and hypersensitive response during the barley-powdery mildew interaction. *The Plant Journal* **11**: 1187–1194.

Urs RR, Roberts PD, Schultz DC. 2006. Localisation of hydrogen peroxide and peroxidase in gametophytes of *Ceratopteris richardii* (C-fern) grown in the presence of pathogenic fungi in a gnotobiotic system. *Annals of Applied Biology* **149**: 327–336.

Van't Hof J. 1985. Control points within the cell cycle. In: Bryant JA, Francis D**.** eds. *The cell division cycle in plants.* Cambridge: Cambridge University Press, 1–13.

Wei Y, Mizzen CA, Cook RG, Gorovsky MA, Allis CD. 1998. Phosphorylation of histone H3 at serine 10 is correlated with chromosome condensation during mitosis and meiosis in *Tetrahymena*. *Proceedings of the National Academy of Sciences, USA* **95**: 7480–7484.

Weingartner M, Criqui MC, Mészáros T, *et al* 2004. Expression of a nondegradable cyclin B1 affects plant development and leads to endomitosis by inhibiting the formation of phragmoplast. *The Plant Cell* **16**: 643–657.

Weinreich M, Palacios DeBeer MA, Fox CA. 2004. The activities of eukaryotic replication origins in chromatin. *Biochimica et Biophysica Acta* **1677**: 142–157.

Żabka A, Polit JT, Maszewski J. 2010. Inter- and intrachromosomal asynchrony of cell division cycle events in root meristem cells of *Allium cepa*: possible connection with gradient of cyclin B-like proteins. *Plant Cell Reports* **29**: 845–856.

Zink D. 2006. The temporal program of DNA replication: new insights into old questions. *Chromosoma* **115**: 273–287.